Conversion of the 2,2,6,6-Tetramethylpiperidine Moiety to a 2,2-Dimethylpyrrolidine by Cytochrome P450: Evidence for a Mechanism Involving Nitroxide Radicals and Heme Iron

Wenji Yin, Kaushik Mitra, Ralph A. Stearns, Thomas A. Baillie, and Sanjeev Kumar*

Department of Drug Metabolism, Merck Research Laboratories, P.O. Box 2000, Rahway, New Jersey 07065

Received October 30, 2003; Revised Manuscript Received February 3, 2004

ABSTRACT: Earlier we described a novel cytochrome P450 (CYP) catalyzed metabolism of the 2,2,6,6-tetramethylpiperidine (2,2,6,6-TMPi) moiety in human liver microsomes to a ring-contracted 2,2-dimethylpyrrolidine (2,2-DMPy) [Yin, W., et al. (2003) *Drug Metab. Dispos. 31*, 215−223]. In the current report, evidence is provided for the involvement of 2,2,6,6-TMPi hydroxylamines and their one-electron oxidation products, the nitroxide radicals, as intermediates in this pathway. Nitroxide radicals could be converted to their corresponding 2,2-DMPy metabolites by "inactivated CYP3A4", as well as by a number of other heme proteins and hemin, suggesting that this is a heme-catalyzed process. The conversion of nitroxide radicals to the 2,2-DMPy products by CYP3A4 or hemin was accompanied by the generation of acetone in incubations, providing evidence that the three-carbon unit from 2,2,6,6-TMPi was lost as acetone. With one model 2,2,6,6-TMPi nitroxide radical, evidence for an alternate pathway, which resulted in the formation of an intermediate that incorporated two oxygen atoms from water of the incubation medium before collapsing to the 2,2-DMPy product, was also obtained. To account for both pathways, a mechanism involving interaction of the nitroxide radicals with heme iron (Fe^{III}), followed by a homolytic scission of the N−O bond and transfer of the nitroxide oxygen to heme iron to form a perferryl−oxygen complex, is proposed. The nitrogen-centered 2,2,6,6-TMPi radical thus formed then precipitates the contraction of the piperidine ring via C2−C3 bond cleavage, and the resulting product further oxidizes to an exocyclic iminium ion (by the perferryl−oxygen complex); the latter may undergo capture by water from the incubation medium and eliminate the three-carbon unit via N-dealkylation. It remains to be determined whether this novel interaction of nitroxide radicals with heme iron has any relevance in regard to the known biological properties of these stable radical species.

Piperidine derivatives are encountered widely in medicinal chemistry since this heterocycle often enhances drug potency due to the introduction of basicity, lipophilicity, or both. However, the piperidine moiety frequently serves as a metabolic "soft spot" in that extensive oxidation may occur on one or other of the carbon atoms α to the ring nitrogen, leading to the formation of lactam or ring-opened products. This frequently results in poor pharmacokinetic properties for the new drug candidates that contain an unsubstituted piperidine moiety. In addition, chemically reactive iminium ions can be formed from *N*-alkylpiperidines, and these electrophilic species have been postulated to play a role in the toxicity of piperidine-containing xenobiotics via covalent modification of proteins and other cellular nucleophiles (ref *1* and references cited therein). One possible strategy to overcome these drawbacks of the unsubstituted piperidine is to employ a 2,2,6,6-tetramethyl-substituted piperidine moiety (2,2,6,6-TMPi).[1] This strategy has been successful at obtaining improvements in pharmacokinetics and blocking iminium ion formation among our new drug candidates. However, the metabolic fate of the 2,2,6,6-TMPi moiety is not fully understood. In a previous publication, we described

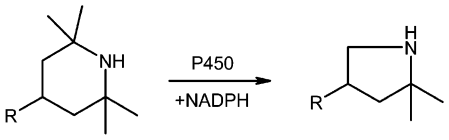

FIGURE 1: Metabolism of the 2,2,6,6-tetramethylpiperidine moiety to a 2,2-dimethylpyrrolidine analogue.

a novel biotransformation of compounds containing the 2,2,6,6-tetramethylpiperidine (2,2,6,6-TMPi) heterocycle in human liver microsomes (Figure 1; *2*). This metabolic pathway results in the loss of three carbon atoms from the 2,2,6,6-TMPi ring and leads to the formation of a ring-contracted 2,2-dimethylpyrrolidine (2,2-DMPy) metabolite. Further, such biotransformation of the 2,2,6,6-TMPi moiety to a 2,2-DMPy was NADPH-dependent and was inhibited by anti-CYP monoclonal antibodies, suggesting that it was a P450-catalyzed reaction. The existence of this metabolic pathway was demonstrated for three compounds that all

* Corresponding author. Phone: 732-594-0261. Fax: 732-594-5390. E-mail: sanjeev_kumar@merck.com.

[1] Abbreviations: CID, collision-induced dissociation; CYP, cytochrome P450; DFX, desferrioxamine; EDTA, ethylenediaminetetraacetic acid; 2,2-DMPy, 2,2-dimethylpyrrolidine; MH^+, protonated molecular ion; MRM, multiple reaction monitoring; MS, mass spectrometry; MS/MS, tandem mass spectrometry; Q-Tof, quadrupole time of flight; SET, single electorn transfer; 2,2,6,6-TMPi, 2,2,6,6-tetramethylpiperidine.

10.1021/bi035944q CCC: $27.50
Published on Web 04/10/2004

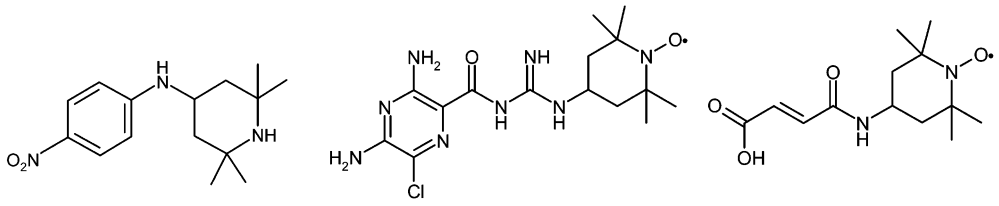

FIGURE 2: Chemical structures of the model 2,2,6,6-tetramethylpiperidine compound **1** and of the two model 2,2,6,6-tetramethylpiperidine nitroxide radical species (**2** and **3**) that were utilized in the current studies.

contained a 2,2,6,6-TMPi moiety but were otherwise structurally distinct. Our recent studies have indicated that 2,2,6,6-TMPi-containing compounds are also metabolized to their corresponding 2,2-DMPy metabolites in rat, dog, and monkey liver microsomes and hepatocytes in vitro as well as in rats in vivo, suggesting that this may be a general metabolic fate of the 2,2,6,6-TMPi moiety in mammalian species. In the current report, we have investigated the mechanistic aspects of this unique metabolic reaction.

It is believed that at least one pathway of P450-catalyzed metabolism of nitrogen-containing aliphatic heterocycles involves a single electron transfer (SET) to form a nitrogen-centered radical cation as the initial step (refs *1* and *3* and references cited therein). This is followed by oxygen recombination (either before or after the second electron transfer) with the radical cation to result in either a hydroxylamine in the case of primary and secondary amines or an *N*-oxide in the case of tertiary amines. Nitrogen-centered radical cations may also deprotonate and rearrange to carbon-centered radicals at positions α to the ring nitrogen; this is followed by oxygen rebound at the α-carbon to result in carbinolamines that can either ring open or undergo further oxidation to lactam metabolites. This α-carbon oxidation is not possible with the 2,2,6,6-TMPi structure because of its inability to deprotonate and form an α-carbon-centered radical. In keeping with this inability of 2,2,6,6-TMPi to undergo α-carbon oxidation, the major metabolites of 2,2,6,6-TMPi-containing compounds were found to be the hydroxylamine derivatives. Interestingly, however, the amounts of the corresponding hydroxylamine metabolites detected in liver microsomal incubations initially increased as a function of incubation time and later appeared to decrease, suggesting that the hydroxylamine derivatives may have undergone secondary metabolism. Concomitant with this decrease in the amounts of the hydroxylamines at later time points was the observation of an increase in the formation of the corresponding 2,2-DMPy metabolites in incubations. For at least some compounds, this latter process continued even after the parent 2,2,6,6-TMPi had been fully depleted, suggesting that it is likely the hydroxylamine, rather than the parent 2,2,6,6-TMPi, that acts as the immediate precursor to the 2,2-DMPy product. It is known that the 2,2,6,6-TMPi hydroxylamine derivatives can be oxidized via two sequential one-electron oxidations to form stable nitroxide radicals and oxoammonium cation species, respectively (*4*, *5*). Thus, we hypothesized that a hydroxylamine-to-nitroxide radical metabolic sequence could possibly be involved in the formation of 2,2-DMPy metabolites from their corresponding 2,2,6,6-TMPi derivatives. To examine this hypothesis, we have examined mechanistic aspects of the metabolism of a model compound **1** containing the 2,2,6,6-TMPi moiety and two model 2,2,6,6-TMPi nitroxide radical derivatives (**2** and **3**) to their corresponding 2,2-DMPy products (Figure 2).

EXPERIMENTAL PROCEDURES

Materials. Compounds **1**−**3** were obtained from the Merck Research Laboratories sample repository. Cytochrome P450 reductase was purchased from Gentest Corp. (Woburn, MA). Hemoglobin, cytochrome *c*, hemin, desferrioxamine (DFX), EDTA, 1,10-phenanthroline, ferrous chloride, ferric chloride, dansylhydrazine, and hydrogen peroxide were purchased from Sigma-Aldrich Chemical Co. (St. Louis, MO). High-purity argon gas was obtained from Airgas (Piscataway, NJ). Isotopically enriched oxygen ($^{18}O_2$, 99% isotopic purity) gas and water ($H_2{}^{18}O$, 95% isotopic purity) were obtained from Isotec (Miamisburg, OH). Microsomes containing recombinant human CYP3A4 were obtained from Drs. Magang Shou and Thomas H. Rushmore (Department of Drug Metabolism, Merck Research Laboratories, West Point, PA). These recombinant CYP3A4-containing microsomes were prepared from Sf21 insect cells infected with recombinant baculoviruses encoding individual CYP cDNAs and cytochrome P450 reductase (*6*). All other reagents were obtained from either Fisher Scientific or Sigma-Aldrich and were of reagent grade.

*LC-MS/MS Assay Methods for the Analysis of Metabolites of **1**−**3**.* When **1** was incubated with microsomes in the presence of NADPH (see below), three different metabolic products were detected including the hydroxylamine and the nitroxide radical derivatives of 2,2,6,6-tetramethylpiperidine and the 2,2-DMPy metabolite. Similarly, upon incubation of **2** and **3** with microsomes (with or without NADPH), the products formed included the corresponding hydroxylamine, the reduction product, 2,2,6,6-tetramethylpiperidine, and the 2,2-DMPy metabolite. To explore the mechanistic interrelationships between these metabolic products, LC-MS/MS-based assay methods were developed to detect these compounds. The structures of the relevant metabolites were first characterized using high-resolution mass spectral measurements on a hybrid quadrupole time-of-flight (Q-Tof) II mass spectrometer (Micromass Corp., Cheshire, U.K.) as described in our earlier publication (*1*).

LC-MS/MS analyses were carried out using a Perkin-Elmer Series 200 HPLC system coupled to a SCIEX API3000 triple quadrupole mass spectrometer (PE Sciex Instruments, Boston, MA). The mass spectrometer was operated in positive ion electrospray mode, and analyte detection was performed using multiple reaction monitoring (MRM). Electrospray voltage and source temperature were 4500 V and 250 °C, respectively, in all cases. Nitrogen was used as the collision gas, and the collision energy was set at 35 eV for all compounds. The mass transitions that were

Table 1: MRM Mass Transitions Employed for the LC-MS/MS Detection of 2,2,6,6-Tetramethylpiperidine (2,2,6,6-TMPi), *N*-Hydroxy-2,2,6,6-tetramethylpiperidine (Hydroxylamine), 2,2,6,6-Tetramethylpiperidine Nitroxide Radical, and 2,2-Dimethylpyrrolidine (2,2-DMPy) Derivatives of **1**−**3**

	mass transition employed for the detection of			
compd	2,2,6,6-TMPi	*N*-hydroxy-2,2,6,6-TMPi (hydroxylamine)	2,2,6,6-TMPi nitroxide radical	2,2-DMPy
1	278 → 149	294 → 149	293 → 149	236 → 149
2	369 → 230	385 → 230	384 → 230	327 → 140
3	255 → 116	271 → 116	270 → 116	213 → 116

employed for monitoring various metabolic products of **1**−**3** are presented in Table 1. Chromatography was carried out using gradient elution on a Betabasic C18 reverse-phase column (100 × 4.6 mm, 5 μm) at an HPLC flow rate of 1 mL/min. Column eluate was split 1:4 between mass spectrometer and waste, respectively. Different HPLC gradient elution profiles were employed for the three compounds to achieve appropriate chromatographic resolution of the compounds of interest. The relative amounts of the metabolite(s) formed under different incubation conditions were compared using metabolite peak areas obtained for the respective samples.

Dependence of Metabolite Formation on the Active Enzyme and/or NADPH. Incubations of **1**−**3** (1 mL volume) with insect cell microsomes containing recombinant CYP3A4 (250 pmol/mL of P450) were conducted at 37 °C in 100 mM potassium phosphate buffer (pH 7.4) containing 10 mM $MgCl_2$ and with or without an NADPH-regenerating system that consisted of 10 mM glucose 6-phosphate, 1 mM $NADP^+$, and 0.7 unit/mL glucose-6-phosphate dehydrogenase. Parallel incubations were conducted with microsomes that were inactivated by immersing in a boiling water bath for 5 min. The substrate concentration for all incubations was 20 μM. Incubations were conducted for 3 h, and the reactions were quenched by the addition of 2 mL of acetonitrile.

Metabolite Formation under Aerobic and Anaerobic Conditions. Incubations of **1**−**3** with recombinant CYP3A4 microsomes were prepared as above; in addition, glucose (5 mM), glucose oxidase (2.5 units/mL), and catalase (20 u/mL) were included in the incubation to rid the incubates of any traces of dissolved oxygen. These incubations were placed in a 37 °C water bath for 15 min either under open atmosphere (aerobic condition) or under an atmosphere of argon (anaerobic condition) before the addition of substrate (20 μM final concentration). Anaerobic conditions were created by multiple alternating cycles of argon purging and vacuum application in an airtight glass assembly. Following the addition of the substrate, incubations were continued for an additional 3 h, at which time the reactions were quenched by the addition of 2 mL of acetonitrile as above. Parallel control incubations were carried out to ensure a lack of metabolism of midazolam to 1′-hydroxymidazolam in the presence of an NADPH-regenerating system via a CYP3A4-mediated reaction in order to verify the existence of anaerobic conditions throughout the incubation period.

Incubations with Model Heme Proteins and Hemin. Stock solutions of cytochrome *c* or bovine methemoglobin (8 mg/mL) were prepared in distilled water. Compounds **1**−**3** were incubated at 37 °C in 100 mM potassium phosphate buffer (pH 7.4) containing 10 mM $MgCl_2$ as above, except that recombinant CYP3A4 was replaced with recombinant P450 reductase (2 mg/mL protein), purified cytochrome *c* (2 mg/mL), or bovine methemoglobin (2 mg/mL).

Compounds **1**−**3** were also incubated with hemin in the above buffer system. Hemin stock solutions were prepared in a dimethyl sulfoxide and water mixture (50:50 v/v). The final concentration of hemin and substrates in the incubation was 1 and 20 μM, respectively.

*Effect of Metal Ion Chelators on the Formation of Metabolites of **2** and **3**.* Incubations of **2** and **3** were carried out as above with recombinant CYP3A4 microsomes without the NADPH-regenerating system. Various concentrations (0, 10, 100, and 1000 μM) of DFX, 1,10-phenanthroline, or EDTA were included in the incubations in order to examine the effect of these metal ion chelators on the formation of 2,2-DMPy products from **2** and **3**.

All incubations were carried out for 3 h. At the end of the incubation period, the reactions were quenched with two volumes of acetonitrile. Samples were centrifuged (10000*g*, 10 min), and the supernatant was separated from precipitated protein and concentrated by evaporation under a gentle stream of nitrogen before analysis by LC-MS/MS.

Effect of Desferrioxamine on the Carbon Monoxide Binding Absorbance Spectrum of CYP3A4 and the Absorbance Spectrum of Hemin. Incubations were prepared as above with recombinant CYP3A4 microsomes either with or without 1 mM DFX. Carbon monoxide binding spectra were then acquired following dithionite reduction on a Shimadzu Model UV-1601 spectrophotometer using the UVProbe version 1.10 software (Shimadzu Scientific Instruments, Columbia, MD) using established procedures (*7*). Similarly, the absorbance spectra of hemin (20 μM) were acquired either with or without 1 mM DFX.

*Detection of Acetone Formed in Incubations of **1**−**3** with Recombinant CYP3A4 Microsomes.* Compounds **1**−**3** at different concentrations (0, 10, 20, 50, and 100 μM) were incubated with recombinant CYP3A4 microsomes in a total volume of 1 mL as above. In addition, **1** was incubated also in the presence of an NADPH-regenerating system. At the end of the 3 h incubation period, a 10 μL aliquot of glacial acetic acid and a 2 μL aliquot of a 300 mM solution of dansylhydrazine were added. The samples were incubated for an additional 30 min period at 37 °C, processed as above, and analyzed immediately for the dansylhydrazone derivative of acetone. Full-scan MS^2 spectra of the dansylhydrazone derivative formed in the above incubations were first acquired and compared to those obtained from an authentic sample prepared by reacting acetone with dansylhydrazine using the procedure described above. This was accomplished using LC-MS on a LCQ-DECA XP ion trap mass spectrometer (Thermo-Finnigan, San Jose, CA) interfaced to a PE Series 200 HPLC system. Chromatography was carried out on a Cogent HPS C18 column (5 μm, 75 × 4.6 mm) using an isocratic mobile phase consisting of a 50:50 mixture of 5 mM ammonium acetate and acetonitrile and containing 0.1% formic acid. The mass spectrometer was operated in the positive ion electrospray mode, with the electrospray voltage, source temperature, and relative collision energy set at 5 kV, 300 °C, and 35%, respectively. Further sample analyses for the measurement of relative amounts of the dansylhydrazone

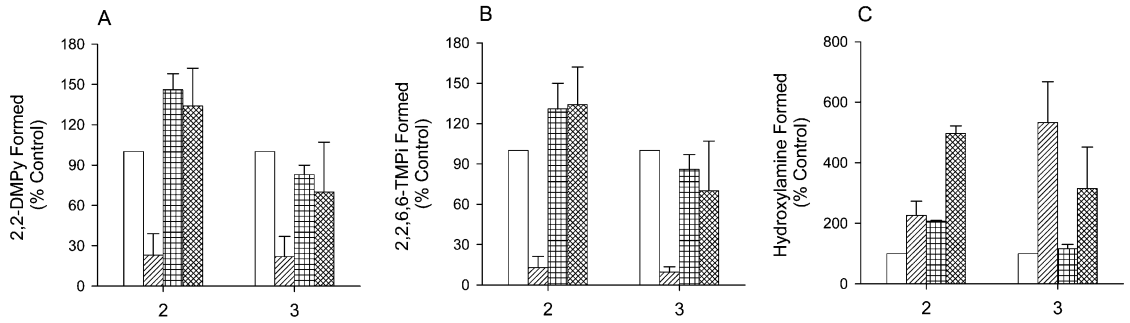

FIGURE 3: Relative extent of formation of the corresponding 2,2-DMPy (A), 2,2,6,6-TMPi (B), and hydroxylamine (C) products upon incubation of **2** and **3** with recombinant CYP3A4 microsomes under different incubation conditions. Incubation conditions: active CYP3A4 with no NADPH and under aerobic atmosphere (□), active CYP3A4 with NADPH and under aerobic atmosphere (▨), boiled CYP3A4 with no NADPH and under aerobic condition (⊞), and active CYP3A4 with no NADPH and under anaerobic atmosphere (⊗).

derivative formed as a function of substrate concentration were carried out using LC-MS/MS on a SCIEX API 3000 mass spectrometer interfaced to a PE Series 200 HPLC system. The mass spectrometer was operated in the positive ion electrospray mode, and HPLC conditions were similar to those described above. Detection of the dansylhydrazone derivative was performed in the MRM mode using an ion transition of *m*/*z* 306 → 171, and peak areas were used to quantify relative amounts of the derivative in various samples. Ion spray voltage, source temperature, and collision energy were set at 4500 V, 300 °C, and 35 eV, respectively.

*Incubations of **2** and **3** with CYP3A4 under an Atmosphere of $^{18}O_2$ or in a Medium Containing $H_2{}^{18}O$.* Compound **2** or **3** (20 μM) was incubated with recombinant CYP3A4 microsomes (250 pmol/mL) as above in the absence of an NADPH-regenerating system. For incubations under an atmosphere of $^{18}O_2$, air was removed from the test tubes by vacuum, followed by purging with $^{18}O_2$ gas using an airtight assembly. The above procedure was repeated at least five times to ensure complete removal of atmospheric air. Reactions were started by the addition of the substrate, and the test tubes were kept sealed to ensure an atmosphere rich in $^{18}O_2$. Parallel control incubations were carried out that monitored the incorporation of ^{18}O into midazolam to form 1′-hydroxymidazolam in the presence of an NADPH-regenerating system via a CYP3A4-mediated reaction in order to verify the existence of an $^{18}O_2$-rich atmosphere throughout the incubation period. In incubations that were to be conducted in the presence of $H_2{}^{18}O$, ~60% of the incubation medium was replaced with $H_2{}^{18}O$; the remaining 40% of the incubation medium consisted of buffer and microsomal preparation and contained $H_2{}^{16}O$. All incubations progressed for a 3 h period at 37 °C, at the end of which reactions were stopped by the addition of acetonitrile and samples processed as above for analysis by LC-MS^n using a LCQ-DECA XP ion trap mass spectrometer.

RESULTS

The effects of various experimental conditions on the relative extent of formation of the corresponding 2,2-DMPy, 2,2,6,6-TMPi (a net three-electron reduction product of nitroxide radicals), and hydroxylamine derivatives upon incubation of **2** and **3** are presented in Figure 3. For **1**, 2,2-DMPy and hydroxylamine metabolites were not detected in incubations other than those conducted in the presence of NADPH and under aerobic conditions; hence, the data for only **2** and **3** are shown in Figure 3. Addition of NADPH to the incubations of **2** and **3** led to a significant reduction in the amounts of the 2,2-DMPy and 2,2,6,6-TMPi products formed, whereas the amounts of the corresponding hydroxylamine were increased. The formation of 2,2-DMPy and 2,2,6,6-TMPi metabolites from nitroxide radicals **2** and **3** was not dependent on the presence of an active CYP3A4 enzyme or of oxygen. Further, since the incubations conducted under anaerobic conditions contained an excess of catalase, a role for hydrogen peroxide in these processes was ruled out. Also, anaerobic incubation conditions appeared to lead to increased reduction of the nitroxide radicals to the corresponding hydroxylamines.

The above data suggested that the conversion of nitroxide radicals **2** and **3** to the corresponding 2,2-DMPy metabolites is nonenzymatic and could possibly be catalyzed either by heme or by trace metal ions in solution. To address the involvement of trace metals in this conversion, **2** and **3** (at 20 μM) were incubated with varying concentrations of Fe^{2+} or Fe^{3+} (1−20 μM). This, however, did not lead to any detectable formation of the corresponding 2,2-DMPy products. To further examine the role of trace metal ions in these processes, incubations of **2** and **3** with recombinant CYP3A4 microsomes were carried out in the presence of various concentrations (10, 100, and 1000 μM) of different metal ion chelators including EDTA, 1,10-phenanthroline, and DFX. EDTA and 1,10-phenathroline did not exhibit any significant effect on the formation of the corresponding 2,2-DMPy and 2,2,6,6-TMPi products from **2** and **3**. DFX, however, caused concentration-dependent inhibition of the formation of these products from both **2** and **3** (Figure 4). Inclusion of DFX up to a concentration of 1 mM did not alter the carbon monoxide binding spectrum of CYP3A4 (data not shown), indicating that the inhibitory effects of DFX were not due to chelation of iron out of the porphyrin system of CYP3A4. The absorbance spectra of hemin (20 μM) either with or without DFX (1 mM) are shown in Figure 5. The changes in absorbance spectra of hemin in the presence of DFX suggest that the latter may alter the immediate environment of the porphyrin system.

To examine the potential role of heme in the conversion of nitroxide radicals to their corresponding 2,2-DMPy analogues, **2** and **3** were incubated with representative heme proteins, such as cytochrome *c*, cytochrome P450 reductase, and bovine methemoglobin, and with hemin. All of the heme proteins examined, as well as hemin alone, were able to

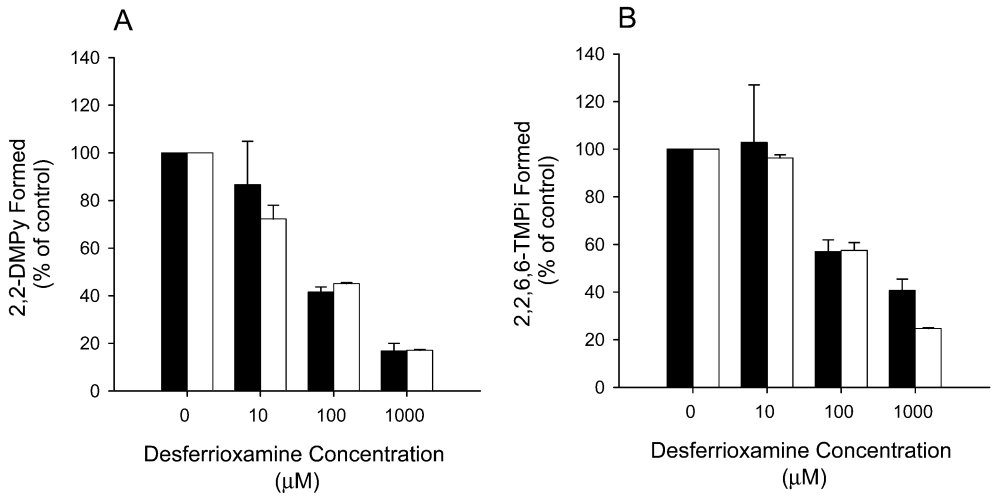

FIGURE 4: Effect of desferrioxamine on the formation of the corresponding 2,2-DMPy (A) and 2,2,6,6-TMPi (B) metabolites upon incubation of the nitroxide radicals **2** (filled bars) and **3** (open bars) with recombinant CYP3A4 microsomes.

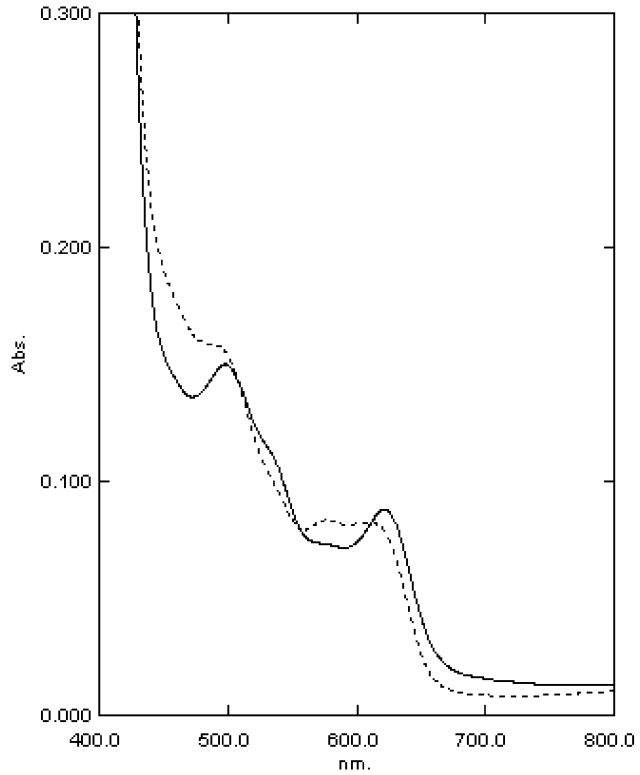

FIGURE 5: Absorbance spectra of hemin (25 μM) alone (solid) or in the presence of 1 mM desferrioxamine (dotted) in the visible wavelength region.

catalyze the conversion of **2** and **3** to their corresponding 2,2-DMPy products (Figure 6). It was interesting to note that the rates of these reactions were the fastest when hemin was used, with essentially all of the nitroxide converted to the ring-contracted pyrrolidine within a 1 h incubation. In contrast, these rates varied widely among the other heme proteins and were also substrate-dependent. This highlights the importance of the apoprotein structure and the nature of the substrate in governing their accessibility to and ease of interaction with heme.

The conversion of nitroxide radicals **2** and **3** to their corresponding 2,2-DMPy products involves the net loss of a mass equivalent to C_3H_6O. To determine if this fragment is lost as acetone, experiments were conducted to detect the formation of acetone in incubations of **2** or **3** with recombinant CYP3A4 and hemin. Figure 7 shows the formation of the dansylhydrazone derivative of acetone in incubations of **2** and **3** with recombinant CYP3A4. For **1**, acetone was detected only when an NADPH-regenerating system was also included in the incubation (data not shown). The identity of the dansylhydrazone derivative of acetone was established by the MS^2 spectra and the suggested fragment ion assignments shown in Figure 7. The fragment ions observed were characteristic of other dansylated derivatives and were identical to those of the standard prepared by reacting acetone with dansylhydrazine under similar conditions. The ions at *m*/*z* 170 and 172 are formed via cleavage of the C−S bond with charge retention on the dimethylaminonaphthyl structure, whereas the ion at *m*/*z* 171 is a radical cation that appears to originate via a modified McLafferty rearrangement of a hydrogen atom from the carbon atom attached to the nitrogen toward the naphthylamine core (*8*, *9*). Similarly, ions at *m*/*z* 234 and 236 appear to be formed via cleavage of the N−S bond with charge retention on the dimethylaminonaphthylsulfonyl nucleus. Further, the mass spectral peak intensities of this dansylhydrazone derivative in incubations increased in a proportional manner as the concentration of **2** or **3** was increased from 20 to 100 μM.

In incubations of **2** with recombinant CYP3A4 and hemin, we detected the heme-dependent formation of a trace level metabolite (denoted as M399 hereafter) with a molecular ion (MH^+ species) at *m*/*z* 399. The MS^2 spectra of this metabolite resulted in a fragment ion at *m*/*z* 327 (MH^+ ion of the 2,2-DMPy metabolite of **2**); sequential MS^3 fragmentation of *m*/*z* 327 gave a mass spectrum identical to that of the 2,2-DMPy metabolite of **2**. Furthermore, when M399 was purified from incubations of **2** with CYP3A4 using HPLC, it fully converted to the 2,2-DMPy metabolite when left at room temperature overnight. This indicated that M399 represents an intermediate in the heme-dependent conversion of **2** to the 2,2-DMPy product. The molecular mass, mass spectral fragmentation, and the decomposition behavior of M399 suggested that it is the carbinolamine shown in Figure 8, with a net incorporation of two oxygen atoms. Incubations conducted under an atmosphere of $^{18}O_2$ ruled out that these oxygen atoms were derived from atmospheric air because no incorporation of ^{18}O occurred into M399 under these

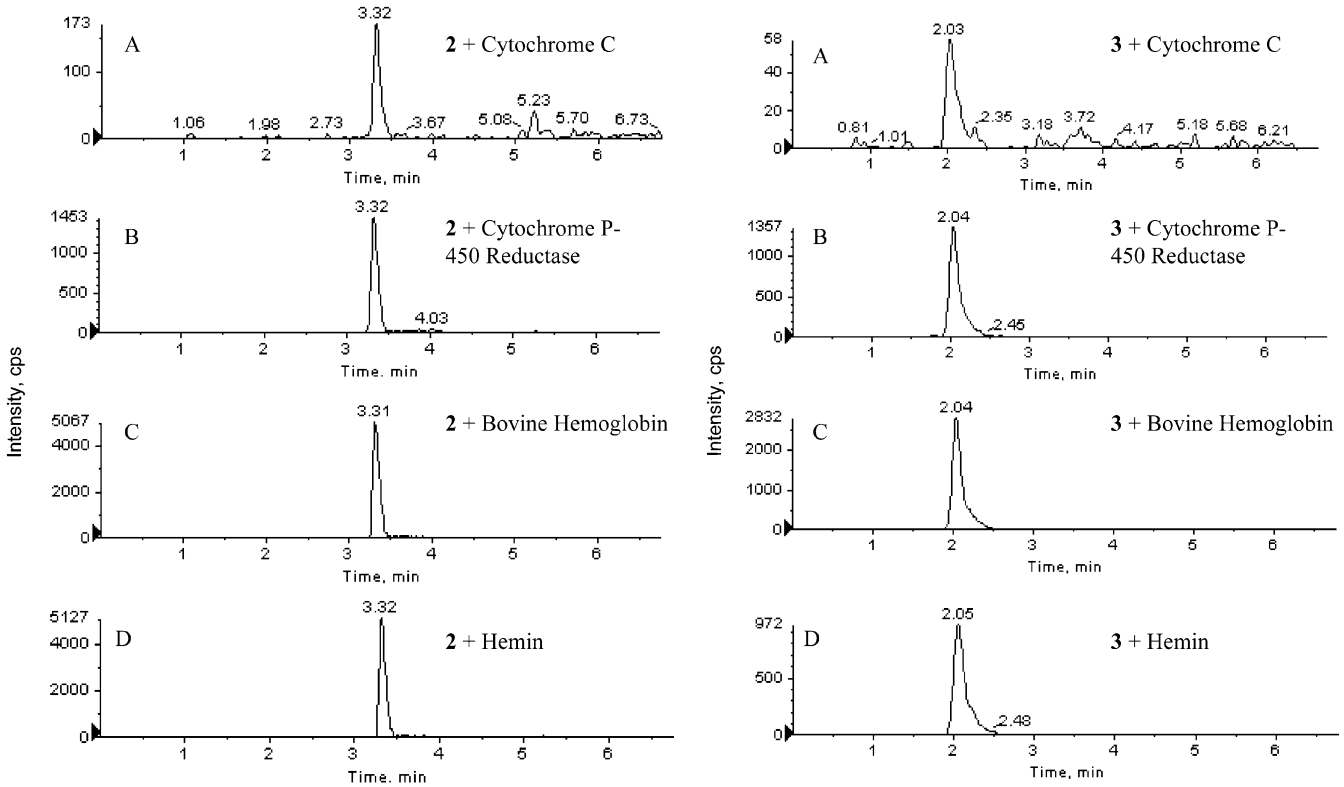

FIGURE 6: Formation of 2,2-DMPy metabolites of **2** (left panel) and **3** (right panel) upon incubation with various model heme proteins and hemin. Reconstructed ion chromatograms for mass transitions of *m*/*z* 327 → 140 and *m*/*z* 213 → 116 are shown for **2** (left panel) and **3** (right panel), respectively, and demonstrate that all heme proteins as well as hemin were capable of converting **2** and **3** to their corresponding ring-contracted 2,2-DMPy derivatives.

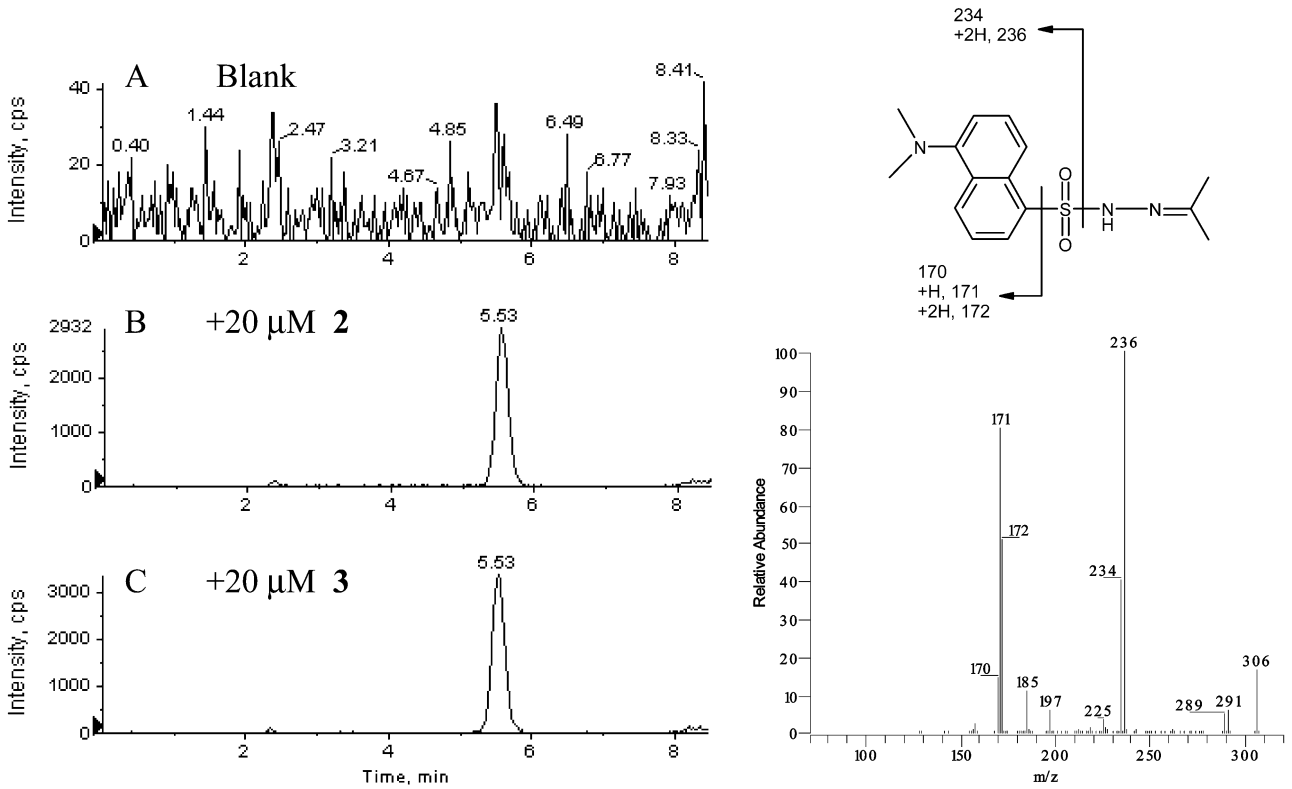

FIGURE 7: Reconstructed ion chromatograms (mass transition *m*/*z* 306 → 171, left panel) showing the generation of acetone upon incubation of **2** and **3** with recombinant CYP3A4 microsomes. Blank incubations did not contain the nitroxide radical **2** or **3**. Acetone was detected as the corresponding hydrazone derivative following derivatization with dansylhydrazine. The right panel shows the MS^2 mass spectrum (products of MH^+ at *m*/*z* 306) of the dansylhydrazone derivative of acetone detected in these incubations and the suggested fragment ion assignments.

conditions. However, when **2** was incubated with recombinant CYP3A4 or hemin in a medium containing 60% $H_2{}^{18}O$, the MS spectrum of M399 showed peaks at *m*/*z* 399, 401, and 403 with relative intensities of approximately 20%,

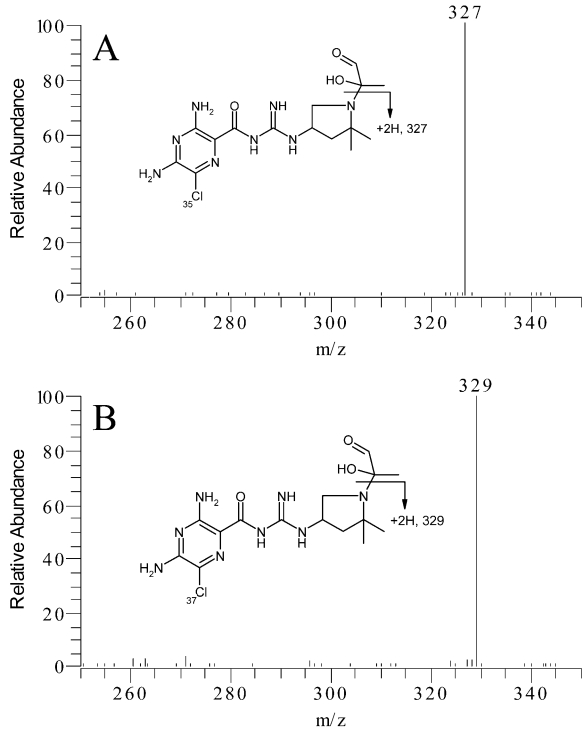

FIGURE 8: MS^2 mass spectra of M399 in incubations of **2** with recombinant CYP3A4 microsomes: (A) products of *m*/*z* 399 (the ^{35}Cl isotope) and (B) products of *m*/*z* 401 (the ^{37}Cl isotope).

100%, and 75%; these relative intensities suggest incorporation of two oxygen atoms, ^{16}O and/or ^{18}O, from the incubation medium in a ratio that is consistent with the relative amounts of $H_2{}^{16}O$ and $H_2{}^{18}O$ present in the medium. Furthermore, the MS^2 spectrum of the ion at *m*/*z* 403 gave a major fragment ion at *m*/*z* 327 (Figure 9C), suggesting that a large fraction of the peak intensity at this mass was derived from the metabolite that had incorporated two ^{18}O atoms from the incubation medium.

In the above incubations of **2** with recombinant CYP3A4 microsomes or hemin, in addition to the hydroxylamine, a second product (denoted as M385 hereafter) with a MH^+ ion at *m*/*z* 385 was detected. From the relative intensities of the MH^+ ions at *m*/*z* 385 and 387, it was clear that this metabolite did not incorporate ^{18}O atoms to any significant extent irrespective of whether the incubations were conducted under an atmosphere of $^{18}O_2$ gas or in an incubation medium containing $H_2{}^{18}O$. Further, the formation of this metabolite occurred to a similar extent under anaerobic as well as aerobic conditions. The MS^2 mass spectrum of M385 in comparison to that of the hydroxylamine of **2**, along with relevant fragment ion assignments, is presented in Figure 10. The fragment ion at *m*/*z* 230 in the spectra of both derivatives suggests that the portion of the molecule other than the 2,2,6,6-TMPi moiety is intact in both species and the difference most likely lies in the exact location of the hydroxyl group on the 2,2,6,6-TMPi. Further, as opposed to the hydroxylamine, the MH^+ ion of M385 and its fragment ion, formed via cleavage of the N−C bond between the 2,2,6,6-TMPi moiety and the rest of the molecule, appear to readily lose the elements of water (H_2O) to give rise to ions at *m*/*z* 367 and 138, respectively. This would suggest that the hydroxyl moiety in M385 is most likely located on one of the *gem*-methyl groups as shown in Figure 10 (although the C-3 position of the 2,2,6,6-TMPi cannot be completely ruled out). Regardless, it appears that the oxygen atom in M385 is derived from either intra- or intermolecular migration of the original nitroxide oxygen via the involvement of heme.

DISCUSSION

As demonstrated in our previous publication (*2*), the formation of a 2,2-DMPy metabolite from **1** in liver microsomal incubations was NADPH-dependent and was inhibited by anti-P450 monoclonal antibodies. This indicated that a P450-catalyzed pathway was involved in this overall metabolic transformation. However, detailed investigations presented in this report clearly suggest that this overall metabolic reaction consists of two separate processes. The first involves a net three-electron oxidation of **1** to the corresponding nitroxide radical through P450 catalysis, whereas the second process occurs independent of an active P450 enzyme, NADPH, or aerobic conditions and leads to the conversion of the nitroxide radicals to their corresponding 2,2-DMPy derivatives (data in Figure 3). In fact, the formation of the 2,2-DMPy products from nitroxide radicals **2** and **3** was reduced in the presence of NADPH; this presumably occurs because the nitroxide radical species were efficiently reduced to their corresponding hydroxylamine derivatives under these conditions. Since this reduction in the formation of 2,2-DMPy products occurred despite a considerable increase in the amounts of hydroxylamine derivatives, a role for these latter species as the immediate precursors to the final 2,2-DMPy products is unlikely. The fact that the conversion of **2** and **3** to their corresponding 2,2-DMPy metabolites could be catalyzed by a variety of heme-containing proteins and boiled CYP3A4 strongly suggests that this process is mediated by the heme component of these proteins. This was further substantiated by the formation of the corresponding 2,2-DMPy metabolites upon incubation of **2** and **3** with hemin. Thus, it appears that the 2,2,6,6-TMPi derivatives undergo a P450-catalyzed two-electron oxidation of the piperidine moiety to a hydroxylamine and a further one-electron oxidation of the hydroxylamine to a nitroxide radical, which then interacts with heme and results in the formation of 2,2-DMPy products.

Since the conversion of 2,2,6,6-TMPi nitroxide radicals to 2,2-DMPy metabolites appears to be mediated by heme, the inhibitory effects of DFX on this process are somewhat surprising. It is generally believed that DFX does not chelate iron out of porphyrin systems (*10*, *11*). Consistent with this, incubation of recombinant CYP3A4-containing microsomes with DFX in our studies did not alter the carbon monoxide binding spectrum of the P450 enzyme. Thus, it appears that DFX is able to interact with heme iron such that it becomes unavailable for interaction with the nitroxide radical species in the incubation medium. Changes seen in the visible wavelength absorbance spectrum of hemin in the presence of DFX appear to support such alteration in the immediate environment of heme iron (Figure 5). It is conceivable that DFX can compete with nitroxides for initial binding/interaction with heme iron because it is known to coordinate iron (Fe^{3+}) via its three hydroxylamine moieties, which may bear some similarity with the N−O$^\bullet$ functionality of the nitroxide radical.

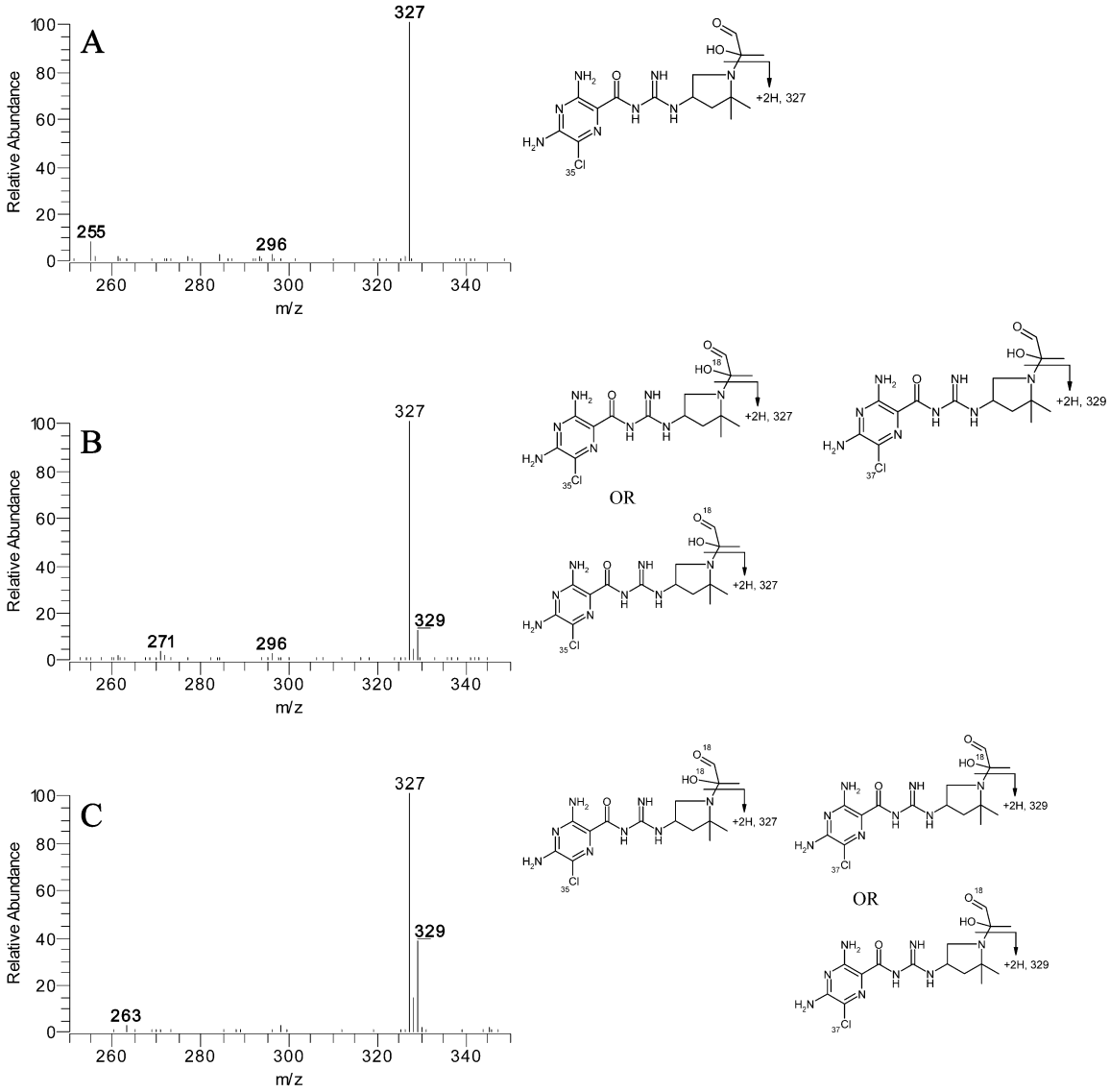

FIGURE 9: MS^2 mass spectra of the M399 metabolite formed upon incubation of **2** with recombinant CYP3A4 microsomes or hemin in an incubation medium containing 60% $H_2{}^{18}O$ and 40% $H_2{}^{16}O$: (A) products of *m*/*z* 399, (B) products of *m*/*z* 401, and (C) products of *m*/*z* 403. The proposed fragment ion assignments establish the incorporation of two ^{16}O and/or ^{18}O atoms into M399 from the incubation medium in a ratio that is consistent with the relative amounts of $H_2{}^{18}O$ and $H_2{}^{16}O$ present.

The heme-catalyzed conversion of the nitroxide radical species to their corresponding 2,2-DMPy derivatives is intriguing and raises questions about the exact chemistry involved in this process. From the data obtained on the formation of acetone and the detection of the M399 metabolite in incubations of nitroxide radicals with hemin or CYP3A4, at least two separate pathways can be envisioned for the formation of 2,2-DMPy products (Figure 11). In the first pathway (sequence A in Figure 11), interaction of the nitroxide radical with the heme iron (Fe^{3+}) induces a homolytic cleavage of the N−O bond and results in the formation of a nitrogen-centered radical and a heme iron−oxygen complex that is equivalent to compound I of peroxidases. The nitrogen-centered radical then precipitates the homolytic scission of the C2−C3 bond of the 2,2,6,6-TMPi ring and results in the formation of a five-membered heterocycle with an N-linked carbon-centered isopropyl radical IV. The compound I-like species can then abstract an electron (from the nitrogen atom of the 2,2-DMPy moiety) and lead to the formation of an iminium cation derivative V (Figure 11, reaction sequence A) which undergoes capture by water to form the hemiaminal VI. The latter species can then N-dealkylate via the loss of the acetone and result in the formation of the 2,2-DMPy metabolite. The formation of acetone in amounts that are proportional to the nitroxide radical concentration in incubations with CYP3A4 or hemin is consistent with this proposed pathway.

The detection of the M399 metabolite that converts spontaneously to the corresponding 2,2-DMPy species clearly represents a second pathway for the formation of the latter product in incubations of **2** with recombinant CYP3A4 or hemin. Furthermore, incubations of **2** with CYP3A4 that were conducted in an atmosphere of $^{18}O_2$ gas or in a medium containing $H_2{}^{18}O$ clearly indicate that the M399 metabolite most likely is a hemiaminal species as shown in Figures 8 and 9 and both of its oxygen atoms are derived from the incubation medium. Figure 11 (reaction sequence B) depicts a potential route that could result in the incorporation of two oxygen atoms from the incubation medium into M399. The 2,2-DMPy derivative with an N-linked isopropyl radical IV may also undergo oxidation via hydrogen abstraction from the terminal methyl group by the compound I-like species

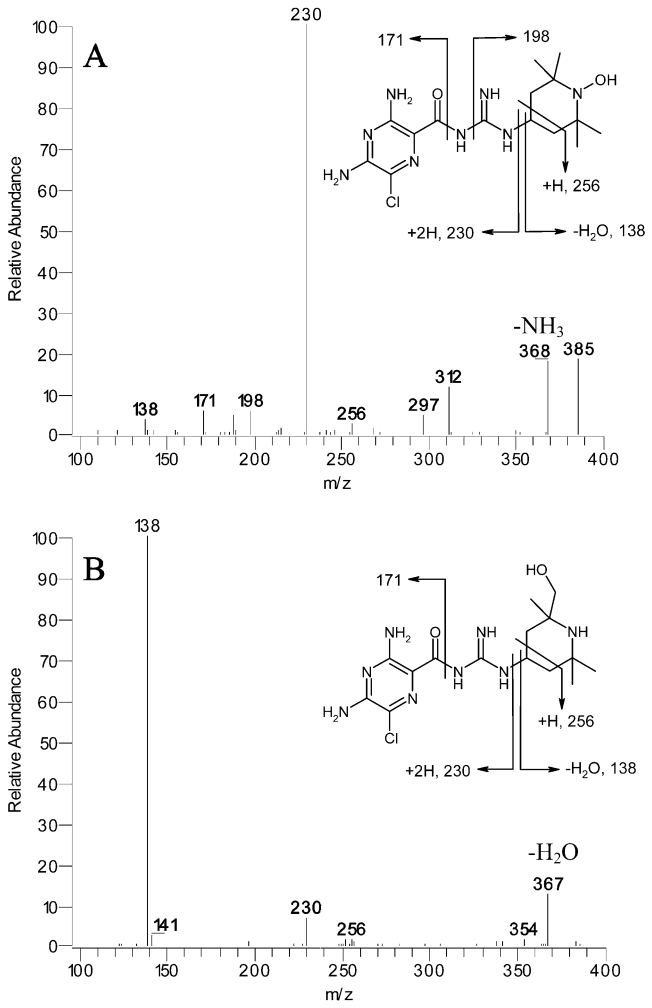

FIGURE 10: MS^2 spectra of the hydroxylamine (A) and M385 (B) metabolites formed in incubations of **2** with recombinant CYP3A4 microsomes or hemin. Relevant fragment ion assignments are also depicted. The exact location of the hydroxyl group of M385 is not known, and the structure drawn only represents the most likely possibility.

that is formed via transfer of the oxygen atom from the nitroxide radical to heme to form the enamine intermediate VII and ferryloxo species equivalent to compound II. Although the enamine VII may convert to the iminium cation V and contribute to reaction sequence A, it can also react with compound II to form the heme-linked radical intermediate VIII, which in turn can result in the formation of an epoxide intermediate IX by losing a single electron (to either heme or other components in the incubation). This epoxide can react with water of the incubation medium to form hemiaminal X, which exists in equilibrium with the iminium cation XI; the latter in turn can easily incorporate another atom of oxygen from the water of the incubation medium to form hemiaminal XII (structurally equivalent to X). The hemiaminal XII will then either directly N-dealkylate via the loss of the side chain as hydroxyacetone or may undergo a (heme-catalyzed) two-electron oxidation of the terminal hydroxyl group to an aldehyde to form XIII (M399), which will lose the side chain as α-ketopropionaldehyde; both of these processes will result in the formation of the 2,2-DMPy product. Interestingly, we only observed XIII in our incubations of **2** with recombinant CYP3A4 or hemin and not its two-electron-reduced version XII. Possible reasons for this may be that either XIII N-dealkylates and converts to the 2,2-DMPy product less efficiently relative to XII (as a result of the decreased basicity of nitrogen because of the presence of a β-carbonyl) or XII is rapidly oxidized to XIII under the conditions of these incubations.

The interaction of nitroxide radicals with heme appears to parallel the interaction of aryldimethylamine *N*-oxides with P450 heme or other model porphyrin biomimetics (*12*−*15*). It has been suggested that the aryldimethylamine *N*-oxides can transfer the oxygen atom to the iron porphyrin system via either a heterolytic or a homolytic scission of the N−O bond; the former would result in the formation of the tertiary amine and a formal Por-Fe^{V}═O species (perferryl iron−oxygen complex equivalent to compound I of peroxidases) whereas the latter would form an aminium radical cation and a formal Por-Fe^{IV}═O species (ferryl iron−oxygen complex equivalent to compound II of peroxidases). In the first instance, the Por-Fe^{V}═O species leads to the hydroxylation of the carbon α to the nitrogen and eventually results in N-demethylation of the tertiary amine to a *N*,*N*-arylmonomethylamine. In the second case, the aminium radical undergoes deprotonation and rearranges to an α-carbon-centered radical along with the formation of a formal Por-Fe^{IV}−OH species; this is followed by radical recombination that completes the α-carbon hydroxylation and the N-dealkylation sequence. Since these tertiary amine *N*-oxides are able to support only intramolecular oxidation reactions that lead to the conversion of the aryldimethylamine *N*-oxide to an arylmonomethylamine (net N-dealkylation) without any detectable oxidation of the other added substrates, it has been suggested that only homolytic cleavage of the N−O bond occurs to generate an aminium radical cation and an oxidant species that is the equivalent of compound II which cannot support formal two-electron oxidations (*14*−*16*). However, at least with one biomimetic porphyrin system, *meso*-(tetraphenylporphinato)iron(III) chloride (TPPFe^{III}Cl), it seems possible to support the two-electron oxidation of a number of substrates including epoxidation of alkenes and hydroxylation of alkanes by utilizing *p*-cyanodimethylaniline *N*-oxide as the oxygen donor (*12*). Thus, it appears that the ability of tertiary amine *N*-oxides to support intermolecular oxidation reactions catalyzed by P450 or its chemical biomimetics may depend on the proximity or orientation of the substrate in relation to heme and also upon the rate of dissociation of the heme−oxygen donor complexes; thus, in general, the intramolecular transfer of the heme-bound oxygen may be more favored. In our studies with the two nitroxide radicals (**2** and **3**) and with TEMPO, we have observed that, similar to tertiary amine *N*-oxides, nitroxide radicals were not able to support the oxidation of midazolam and diclofenac by recombinant CYP3A4 and CYP2C9, respectively (data not shown). However, in the case of **2**, the formation of the M385 derivative that was presumably formed via intramolecular transfer of the oxygen (although intermolecular reactions cannot be ruled out) was observed upon its incubation with recombinant CYP3A4 or hemin. The mass spectral fragmentation data indicated that M385 was most likely oxidized at one of the gemimal methyl groups. It is interesting to note that some of the hydrogens of the geminal methyl groups of the 2,2,6,6-TMPi moiety are within the same range of distance from the piperidine nitrogen (and potentially the heme-bound oxygen) as the

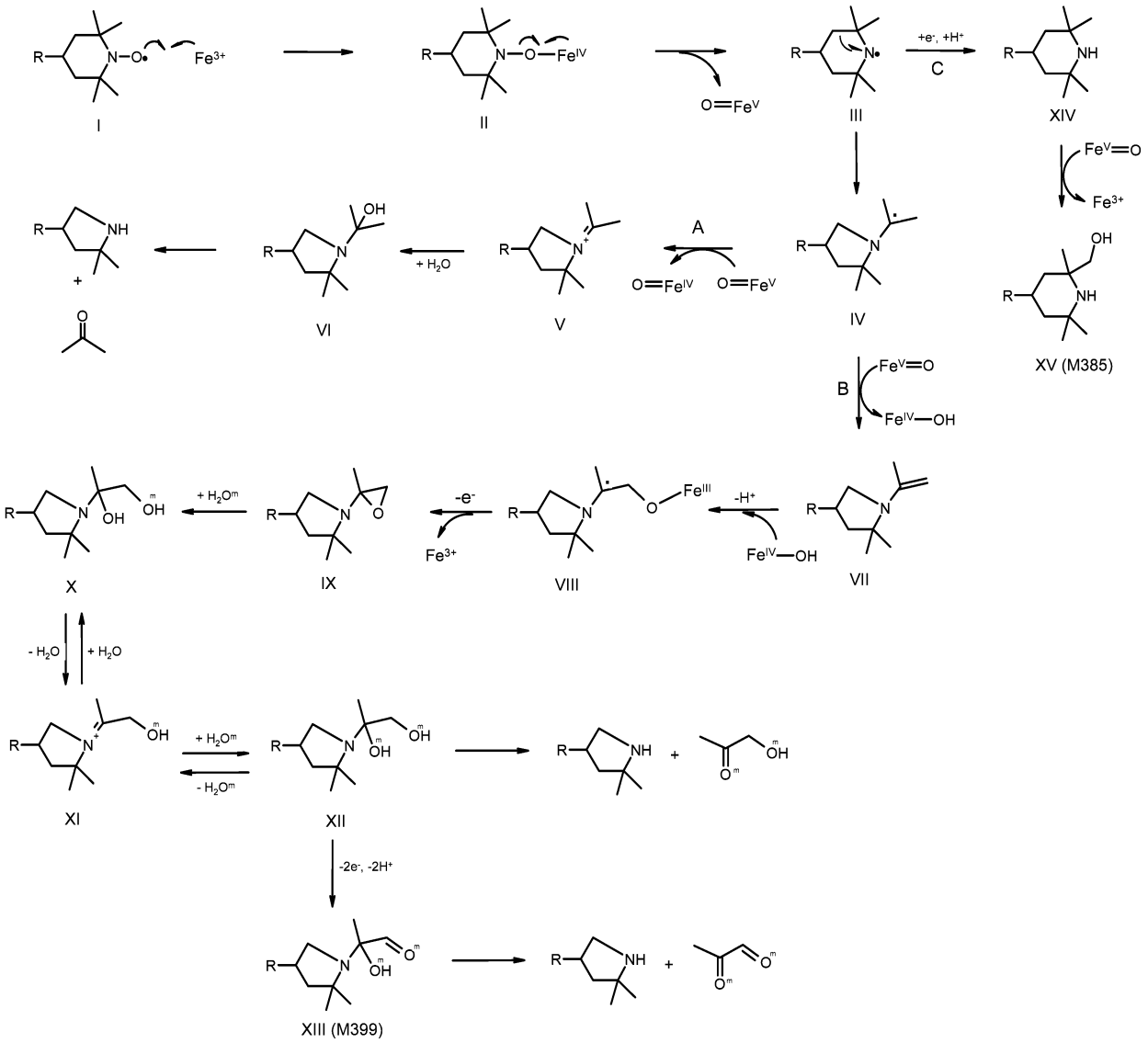

FIGURE 11: Some possible mechanisms for the conversion of the 2,2,6,6-tetramethylpiperidine nitroxide radical to the corresponding 2,2-dimethylpyrrolidine product via the involvement of heme iron. The first pathway (A) is based on the generation of acetone in the incubation, whereas the second (B) provides a possible explanation for the incorporation of two oxygen atoms into the molecule from water of the incubation medium before its final degradation to 2,2-dimethylpyrrolidine. The superscript m denotes oxygen atoms derived from water of the incubation medium. Reaction sequence C provides a potential route to the heme-dependent reduction of the nitroxide radical to 2,2,6,6-TMPi and ultimately to the M385 product.

hydrogens of a methyl group directly attached to the nitrogen as in the case of a tertiary amine (2.4 vs 2.0 Å, respectively). Thus, it is conceivable that M385 is formed via the intramolecular transfer of the nitroxide oxygen through the involvement of heme iron as shown in Figure 11 (reaction sequence C). A second possibility is depicted in Figure 12, which suggests that interaction of the hydroxylamine derivative of **2** with Fe^{III} heme leads to the formation of a perferryl iron−oxygen complex that is equivalent to compound I of peroxidases and can hydroxylate the 2,2,6,6-TMPi moiety at positions other than the nitrogen. This reaction sequence also provides a potential route to the simultaneous heme-dependent reduction of the nitroxide radical and/or the hydroxylamine to the corresponding 2,2,6,6-TMPi. However, the fact that the formation of the 2,2,6,6-TMPi product was reduced in the presence of NADPH when the amounts of the corresponding hydroxylamine were substantially increased (Figure 3) would argue against the mechanism outlined in Figure 12. These observations also appear to support the mechanism depicted in reaction sequence B of Figure 11 for the formation of 2,2-DMPy metabolites in that the heme-dependent intra- or intermolecular transfer of the nitroxide oxygen may occur either with or without the contraction of the six-membered 2,2,6,6-TMPi ring to a five-membered 2,2-DMPy heterocycle. Interestingly, neither its oxidized derivatives (similar to M385) nor reaction sequence B was detected when **3** was incubated with recombinant CYP3A4 or hemin. This further serves to highlight the potential impact of the nature of the substrate and its interaction with heme (and also its orientation within the active site of the enzyme when the enzyme-based experimental systems are used) on the ultimate fate of the "oxygen" that is transferred from the nitroxide radical to the porphyrin iron.

Nitroxides are widely believed to have antioxidant properties and have been shown to inhibit oxidative damage imposed by several different types of insult in cell cultures, isolated organs, and whole animals (*17*−*23*). Several mech-

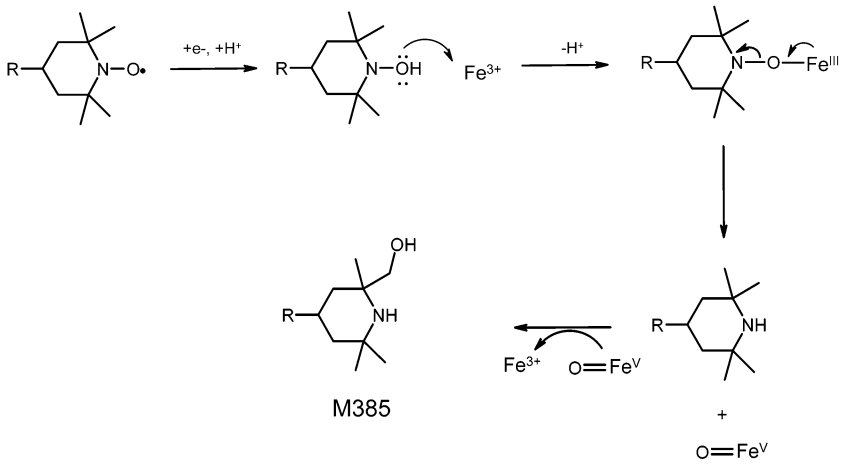

FIGURE 12: A proposed mechanism for the reduction of the 2,2,6,6-TMPi nitroxide radical species to the corresponding 2,2,6,6-TMPi and formation of the M385 metabolite via the involvement of heme iron.

anisms underlying the antioxidant activity have been proposed, including the oxidation of redox-active transition state metal ions and ion complexes (*17*, *18*, *24*), detoxification of xenobiotic-derived semiquinones (*25*), termination of radical chain reactions (*26*, *27*), catalytic removal of superoxide anion $O_2^{\bullet -}$ (*4*), and stimulation of catalase-like activity of heme proteins (*5*, *28*). At least some of the antioxidant activity of nitroxides stems from their ability to reduce, in a catalytic manner, the hypervalent heme species (e.g., oxoferryl complexes) that are formed during various metabolic processes or via reaction of heme proteins with H_2O_2 (*5*, *28*−*30*). This catalytic property of nitroxides arises from their ability to be readily oxidized to a one-electron oxidized form, the oxoammonium cation, by the hypervalent heme complexes. The oxoammonium cation in turn can be reduced via a variety of cellular one- or two-electron reductants to either regenerate the nitroxide radical or be converted to the hydroxylamine, respectively (*4*, *5*, *28*). The hydroxylamine species can then undergo a one-electron oxidation back to the nitroxide radical at the level of cytochrome *c* oxidase and complete the catalytic cycle (*31*). The apparent interaction of 2,2,6,6-TMPi nitroxide radicals with Fe^{III} heme that is involved in the formation of the 2,2-DMPy metabolites (and thus leads to the irreversible consumption of nitroxide radicals) in our current studies appears to be distinct from the above-described catalytic interaction of these radical species with the hypervalent iron−oxo complexes of heme. The role of this novel process in the biological properties of nitroxide radicals is unclear at present and warrants further investigation. It has been shown that, under certain circumstances, nitroxide radicals may act as prooxidants and may potentiate oxidative damage and/or induce proapoptotic stimuli (*32*−*35*). In the mechanisms proposed in Figure 11 for the formation of 2,2-DMPy metabolites from 2,2,6,6-TMPi nitroxide radicals, the reaction sequence involves the formation of a number of free radical and hypervalent heme iron intermediates. It is possible that some of these species may be involved in the prooxidant properties of nitroxide radicals. Regardless, it appears that the disposition of nitroxide radicals and their interactions with cellular macromolecules are highly complex and not fully understood. A better appreciation of these phenomena is essential in order to fully grasp the diverse biological effects of such compounds.

In conclusion, we have identified a unique interaction of 2,2,6,6-TMPi nitroxide radicals with Fe^{III} heme iron that leads to the irreversible conversion of these six-membered-ring piperidinyl radical species to ring-contracted 2,2-DMPy products. The three-carbon unit from the tetramethylpiperidine ring system is lost as acetone and, at least in one case, most likely also as a dicarbonyl (α-ketopropionaldehyde) species. This interaction of nitroxide radicals with heme iron may have other biological implications and requires further investigation.

ACKNOWLEDGMENT

We thank Dr. Richard Tschirret-Guth for assistance with experiments conducted under an anaerobic or $^{18}O_2$-rich atmosphere.

SUPPORTING INFORMATION AVAILABLE

Analytical data on the identity and purity of compounds **1**−**3**. This material is available free of charge via the Internet at http://www.pubs.acs.org.

REFERENCES

1. Castagnoli, N., Jr., Rimoldi, J. M., Bloomquist, J., and Castagnoli, K. P. (1997) Potential metabolic bioactivation pathways involving cyclic tertiary amines and azaarenes, *Chem. Res. Toxicol. 10*, 924−940.
2. Yin, W., Doss, G. A., Stearns, R. A., Chaudhary, A. G., Hop, C. E., Franklin, R. B., and Kumar, S. (2003) A novel P450-catalyzed transformation of the 2,2,6,6-tetramethyl piperidine moiety to a *2*,2-dimethyl pyrrolidine in human liver microsomes: characterization by high-resolution quadrupole-time-of-flight mass spectrometry and ^{1}H NMR, *Drug Metab. Dispos*. *31*, 215−223.
3. Guengerich, F. P. (2001) Common and uncommon cytochrome P450 reactions related to metabolism and chemical toxicity, *Chem. Res. Toxicol*. *14*, 611−650.
4. Krishna, M. C., Grahame, D. A., Samuni, A., Mitchell, J. B., and Russo, A. (1992) Oxoammonium cation intermediate in the nitroxide-catalyzed dismutation of superoxide, *Proc. Natl. Acad. Sci. U.S.A. 89*, 5537−5541.
5. Mehlhorn, R. J., and Swanson, C. E. (1992) Nitroxide-stimulated H_2O_2 decomposition by peroxidases and pseudoperoxidases, *Free Radical Res. Commun*. *17*, 157−175.
6. Mei, Q., Tang, C., Assang, C., Lin, Y., Slaughter, D., Rodrigues, A. D., Baillie, T. A., Rushmore, T. H., and Shou, M. (1999) Role of a potent inhibitory monoclonal antibody to cytochrome P-450 3A4 in assessment of human drug metabolism, *J. Pharmacol. Exp. Ther*. *291*, 749−759.
7. Omura, T., and Sato, R. (1962) A new cytochrome in liver microsomes, *J. Biol. Chem*. *237*, 1375−1376.

8. Oprean, R., Roman, L., and Sandulescu, R. (1996) A modified McLafferty rearrangement in the electron impact mass spectra of dansylated amino acid esters, *J. Pharm. Biomed. Anal. 14*, 1031−1035.
9. Dalvie, D. K., and O'Donnel, J. P. (1998) Characterization of polar urinary metabolites by ionspray tandem mass spectrometry following dansylation, *Rapid Commun. Mass Spectrom. 12*, 419−422.
10. Kerberle, H. (1964) The biochemistry of desferrioxamine and its relation to iron metabolism, *Ann. N.Y. Acad. Sci. 199*, 758−768.
11. Carlin, G., Djursater, R., and Arfors, K. E. (1988) Inhibition of heme-promoted enzymatic lipid peroxidation by desferrioxamine and EDTA, *Upsala J. Med. Sci. 93*, 215−223.
12. Shannon, P., and Bruice, T. C. (1981) A novel P-450 model system for the N-dealkylation reaction, *J. Am. Chem. Soc. 103*, 4580−4582.
13. Nee, M. W., and Bruice, T. C. (1982) Use of *N*-oxide of *p*-cyano-*N*,*N*-dimethylaniline as an "oxygen" donor in a cytochrome P-450 model system, *J. Am. Chem. Soc. 104*, 6123−6125.
14. Heimbrook, D. C., Murray, R. I., Egeberg, K. D., Sligar, S. G., Nee, M. W., and Bruice, T. C. (1984) Demethylation of *N*,*N*-dimethylaniline and *p*-cyano-*N*,*N*-dimethylaniline and their *N*-oxides by cytochromes $P450_{LM2}$ and $P450_{CAM}$, *J. Am. Chem. Soc. 106*, 1514−1515.
15. Seto, Y., and Guengerich, F. P. (1993) Partitioning between N-dealkylation and N-oxygenation in the oxidation of N,N-dialkylarylamines catalyzed by P450 2B1, *J. Biol. Chem. 268*, 9986−9997.
16. Ortiz de Montellano, P. R. (1995) Oxygen activation and reactivity, in *Cytochrome P450: Structure, Mechanism and Biochemistry* (Ortiz de Montellano, P. R., Ed.) Chapter 8, pp 245−303, Plenum Press, New York.
17. Mitchell, J. B., Samuni, A., Krishna, M. C., DeGraff, W. G., Ahn, M. S., Samuni, U., and Russo, A. (1990) Biologically active metal-independent superoxide dismutase mimics, *Biochemistry 29*, 2802−2807.
18. Mitchell, J. B., DeGraff, W., Kaufman, D., Krishna, M. C., Samuni, A., Finkelstein, E., Ahn, M. S., Hahn, S. M., Gamson, J., and Russo, A. (1991) Inhibition of oxygen-dependent radiation-induced damage by the nitroxide superoxide dismutase mimic, tempol, *Arch. Biochem. Biophys. 289*, 62−70.
19. Hahn, S. M., Tochner, Z., Krishna, C. M., Glass, J., Wilson, L., Samuni, A., Sprague, M., Venzon, D., Glatstein, E., Mitchell, J. B., and Russo, A. (1992) Tempol, a stable free radical, is a novel murine radiation protector, *Cancer Res. 52*, 1750−1753.
20. Gelvan, D., Saltman, P., and Powell, S. R. (1991) Cardiac reperfusion damage prevented by a nitroxide free radical, *Proc. Natl. Acad. Sci. U.S.A. 88*, 4680−4684.
21. Karmeli, F., Eliakim, R., Okon, E., Samuni, A., and Rachmilewitz, D. (1995) A stable nitroxide radical effectively decreases mucosal damage in experimental colitis, *Gut 37*, 386−393.
22. Samuni, A., Karmeli, F., Moshen, M., and Rachmilewitz, D. (1999) Mechanisms underlying gastric antiulcerative activity of nitroxides in rats, *Free Radical Res. 30*, 133−140.
23. Xavier, S., Yamada, K., Samuni, A. M., Samuni, A., DeGraff, W., Krishna, M. C., and Mitchell, J. B. (2002) Differential protection by nitroxides and hydroxylamines to radiation-induced and metal ion-catalyzed oxidative damage, *Biochim Biophys Acta 1573*, 109−120.
24. Samuni, A., Goldinger, D., Aronovitch, J., Russo, A., and Mitchell, J. B. (1991) Nitroxides block DNA scission and protect cells from oxidative damage, *Biochemistry 30*, 555−561.
25. DeGraff, W., Hahn, S. M., Mitchell, J. B., and Krishna, M. C. (1994) Free radical modes of cytotoxicity of adriamycin and streptonigrin, *Biochem. Pharmacol. 48*, 1427−1435.
26. Nilsson, U. A., Olsson, L. I., Carlin, G., and Bylund-Fellenius, A. C. (1989) Inhibition of lipid peroxidation by spin labels. Relationships between structure and function, *J. Biol. Chem. 264*, 11131−11135.
27. Lurie, Z., Offer, T., Russo, A., Samuni, A., and Nitzan, D. (2003) Do stable nitroxide radicals catalyze or inhibit the degradation of hyaluronic acid?, *Free Radical Biol. Med. 35*, 169−178.
28. Krishna, M. C., Samuni, A., Taira, J., Goldstein, S., Mitchell, J. B., and Russo, A. (1996) Stimulation by nitroxides of catalase-like activity of hemeproteins. Kinetics and mechanism, *J. Biol. Chem. 271*, 26018−26025.
29. Yamaguchi, T., Nagano, T., and Kimoto, E. (1984) Oxidation of nitroxide radicals by the reaction of hemoglobin with hydrogen peroxide, *Biochem. Biophys. Res. Commun. 120*, 534−539.
30. De Bono, D., Yang, W. D., and Symons, M. C. (1994) The effect of myoglobin on the stability of the hydroxyl-radical adducts of 5,5-dimethyl-1-pyrolline-*N*-oxide (DMPO), 3,3,5,5-tetramethyl-1-pyrolline-*N*-oxide (TMPO) and 1-alpha-phenyl-*tert*-butyl nitrone (PBM) in the presence of hydrogen peroxide, *Free Radical Res. 20*, 327−332.
31. Chen, K., Glockner, J. F., Morse, P. D., and Swartz, H. M. (1989) Effects of oxygen on the metabolism of nitroxide spin labels in cells, *Biochemistry 28*, 2496−2501.
32. Offer, T., Russo, A., and Samuni, A. (2000) The pro-oxidative activity of SOD and nitroxide SOD mimics, *FASEB J. 14*, 1215−1223.
33. Gariboldi, M. B., Rimoldi, V., Supino, R., Favini, E., and Monti, E. (2000) The nitroxide tempol induces oxidative stress, p21-(WAF1/CIP1), and cell death in HL60 cells, *Free Radical Biol. Med. 29*, 633−641.
34. Metodiewa, D., Skolimowski, J., Kochman, A., and Koceva-Chyla, A. (2000) The paradoxical apoptotic effects of novel nitroxide antioxidants on Yoshida sarcoma cells in vivo: a commentary, *Anticancer Res. 20*, 2593−2599.
35. Glebska, J., Skolimowski, J., Kudzin, Z., Gwozdzinski, K., Grzelak, A., and Bartosz, G. (2003) Pro-oxidative activity of nitroxides in their reactions with glutathione, *Free Radical Biol. Med. 35*, 310−316.

BI035944Q